Neutron Powder Diffraction study of the Magnetic Ionic Liquid Emim[FeCL$_4$] and its deuterated phase

You may also be interested in:

Effect of Ionic Liquid (emim BF4) on the Dispersion of Gold Nanoparticles
Mohamed R. Tchalala, Dalaver H. Anjum and Sahraoui Chaieb

Long-range magnetic ordering in magnetic ionic liquid: Emim[FeCl4]
I de Pedro, D P Rojas, J Albo et al.

Activation of lipase in ionic liquids by modification with comb-shaped poly(ethylene glycol)
Kazunori Nakashima, Jun Okada, Tatsuo Maruyama et al.

Enhanced thermoelectric power of single-wall carbon nanotube film blended with ionic liquid
Shohei Horike, Masahiro Misaki, Yasuko Koshiba et al.

Increasing the intensity of protonated secondary ions in time-of-flight secondary ion mass spectrometry using a proton-conducting ionic liquid, diethylmethylammonium trifluoromethanesulfonate
Yukio Fujiwara and Naoaki Saito

In situ Raman study of dissolved carbon-dioxide induced changes of imidazolium-based ionic liquids
Takashi Makino

Gigahertz elastic properties of cryoprotective aqueous solutions of inonic liquids and trehalose
Haruki Takayama, Tomohiko Shibata, Yuto Kuroda et al.

Nonlinear properties and collisional spectra in hydrogen-(heavy) noble-gas-atom mixtures
Waldemar Gaz, Tadeusz Bancewicz, George Maroulis et al.

Neutron Powder Diffraction study of the Magnetic Ionic Liquid Emim[FeCl₄] and its deuterated phase

A. García-Saiz[1], I. de Pedro[*1], L. Fernández Barquín[1], M.T. Fernández-Díaz[2] J. A. Blanco[3] and J. Rodríguez Fernández[1]

[1] CITIMAC, Facultad de Ciencias, Universidad de Cantabria, Santander 39005, Spain.
[2] Institut Laue-Langevin, BP 156X, F-38042 Grenoble Cedex, France
[3] Departamento de Física, Universidad de Oviedo, 33007 Oviedo, Spain

E-mail: depedrovm@unican.es

Abstract. A magnetic ionic liquid comprising 1-ethyl-3 methylimidazolium (Emim) cations and tetraclhoroferrate(III) ($FeCl_4$) anions and its deuterated phase were synthetized and characterized magnetically. In both materials, the low temperature dependence of the magnetic susceptibility presents a maximum (around 4 K) related to an antiferromagnetic ordering, but the ordering temperatures are slightly shifted and the curves display different shapes. In addition, the magnetization of the deuterated phase tends to saturate at higher values than that corresponding to the non-deuterated analogue. A comparison of the neutron diffraction patterns above and below the magnetic transition clearly shows that the crystal and magnetic structures of these materials are different. Therefore, the present findings clearly prove that the magnetic exchange interactions that induce three-dimensional magnetic ordering are modified after the deuteration process.

1. Introduction

Magnetic ionic liquids (MILs) have received considerable attention among ionic liquids (ILs). The interest is fuelled by the possibility of tuning the materials properties by means of external magnetic fields or using them in the liquid state to produce nanoparticle-free magnetic emulsions and microemulsions [1]. Moreover, MILs can combine magnetic and ILs properties with additional intrinsic thermochromic, magneto-electrochromic or luminescent properties depending on the enclosed paramagnetic ion used [2]. The combinations of different rare-earth (europium, neodymium, dysprosium, etc.) chiral amionacids, bimagnetic ions or heteroanions have been studied for applications such as transport and separation of materials, separation of greenhouse gases (CO_2) through supported magnetic ionic liquids membranes, magnetic surfactants or esterification of oleic acid to biodiesel [3].

MILs have also recently received attention from the experimental and theoretical point of view concerning to non-covalent interactions and cohesion properties [4]. Many groups have focused their studies on the dipole-dipole interactions, and hydrogen bonds within the crystal and molecular structures in order to improve the understanding of these forces, with the aim of tailoring their potential technological applications [5]. Importantly, in MILs with paramagnetic ions, such as those presented here, it is also necessary to investigate other non-covalent interactions, like halogen-halogen

(between the nearest metal complex anions) or anion-π (between the anion and cation) as these forces play an important role in the organization of the structural units [6]. In addition, when these interactions are strong enough, interesting collective electrical and magnetic phenomena can arise, such as ferroelectricity in the bis(imidazolium) pentachloroantimonate (III), $(C_3N_2H_5)_2SbCl_5$ [7], or a three-dimensional (3D) magnetic ordering in MILs based on tetrahaloferrate ions [8, 9]. In this last family, recent research shows that a smaller chain length in the organic cation enhances the efficiency in the transmission of the magnetic interactions resulting in an increase in the Néel temperature, T_N (from $[Bmim]^+$ that shows no 3D magnetic ordering through $[Emim]^+$, with $T_N = 3.8$ K [10], to $[Dimim]^+$, with $T_N = 5.6$ K [11]) [Bmim: 1-butyl-3-methylimidazolium and Dimim: 1,3-dimethylimidazolium]. Moreover, the change of external conditions, like pressure, has a strong influence in the magnetic coupling of $Emim[FeCl_4]$, varying from antiferromagnetic (AF) to ferrimagnetic ordering [12]. In this contribution we focus on ascertaining the nature of the magnetic structure of this last MIL, using neutron diffraction experiments. The presence of H atoms in the cation part (H= 11) of $Emim[FeCl_4]$ predicted low statistics in the neutron diffraction pattern. Therefore, in order to avoid the large incoherent component of the hydrogen, which creates a large continuous background and complicates the structural resolution, we have also prepared the fully deuterated sample, $Emim[FeCl_4]$ d11. Herein, we present the comparative study considering magnetic susceptibility and neutron powder diffraction data.

2. Results and discussion

The zero-field-cooled (ZFC) molar susceptibility (χ_m) at magnetic field of 1 kOe of $Emim[FeCl_4]$ d11 displays a paramagnetic behaviour over most of the temperature range studied, with an effective paramagnetic moment, $\mu_{eff} = 5.70(1)$ μ_B/Fe ion, and a paramagnetic Curie temperature, $\theta_p = -3.0(1)$ K. These data anticipate an overall antiferromagnetic behaviour in good agreement with their non-deuterated phase ($\mu_{eff} = 5.66(1)$ μ_B/Fe ion and and $\theta_p = -2.5(1)$ K) [8, 9]. At low temperatures (see Figure 1), χ_m of $Emim[FeCl_4]$ d11 increases and reaches a maximum at approximately 4.0 K, which suggests the existence of a long-range magnetic ordering. The most striking features of these curves being a small displacement of ordering temperature and the different shape with respect to the non-deuterated phase. These facts indicate that the magnetic coupling is modified with the deuteration process. Moreover, the magnetization of $Emim[FeCl_4]$ d11 tends to saturate above 40 kOe, with higher values than those corresponding to the non-deuterated analogue (M ≈ 4.9 μ_B/Fe ion), and it is near the expected fully-saturated value of 5 μ_B/Fe for Fe (III) ion (see Figure 2). As occurs in the non-deuterated compound, the magnetization shows no-hysteresis, thereby discarding the existence of any ferromagnetic component.
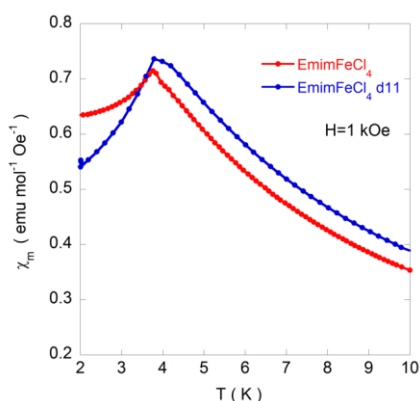

**Figure 1**. Low temperature ZFC magnetic susceptibility for Emin[FeCl₄] and its deuterated phase.
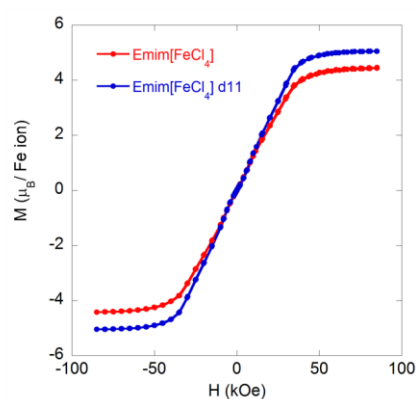
Figure 2. Magnetization of Emin[FeCl₄] and its deuterated phase measured at 2 K.

Neutron powder diffraction patterns of Emim[FeCl$_4$], from 270 to 2 K, and of deuterated analogue at 10 and 2 K were collected on D1B diffractometer at the ILL (λ = 2.52 Å). In these experiments, about 2 g of the sample mass was frozen and then milled before it placing in a cylindrical vanadium container pre-cooled at N$_2$ liquid. The samples were rapidly placed in the cryostat at temperature below the melting point (285K), checking that no preferential orientation was present. The diffraction patterns were collected in the Bragg angular range 5 ≤ 2θ ≤ 70º. The 2D contour plots of the temperature dependence of the neutron diffraction data of the non-deuterated compound is shown in Figure 3). On one hand, a structural phase transition below 210 K is detected in the neutron diffraction patterns, which seems to be stable down to 2 K. This feature could be related to dynamical reorientations of the cations or anions during the cooling process. Therefore, the appearance of a new peak at lower angle regions at 14.5° (d = 10.06 Å) and the splitting of some crystallographic peaks (such as the one located at 2θ ≈ 45°) could be indicative of a loss of symmetry. This issue differs from the data reported for the Dimim[FeCl$_4$] [11], in which the structural phase transition changes the symmetry from P2$_1$ (R.T) to P2$_1$2$_1$2$_1$ at 285 K. Additionally, the presence of extra magnetic signals below 4 K reveals the occurrence of a long-range magnetic ordering compatible with the magnetization results.

The high temperature crystal structure was refined starting from the previously reported single-crystal structure model [13]. The best Rietveld refinement from powder diffraction data at 270 K a framework, which projected along *b* axis, can be described as a stacking of [Edimim]$^+$ and [FeCl$_4$]$^-$ intercalated layers, with Fe···Fe distances larger than 6.5 Å inside the layer [monoclinic space group P2$_1$/c; a = 9.424(3) Å, b = 14.662(4) Å, c = 12.449(9) Å, β = 129.89(2)º , V= 1319.2(4) Å^3]. The anion groups [FeCl$_4$]$^-$, slightly distorted, form subnets in the *a,c* plane with a change of orientation from layer to layer and a displacement of the subnet with respect to the next one. The cations, [Emim]$^+$, also form subnets in the *a,c* plane but are stacked nearly identically above one another, lying parallel to each other along *b* direction (see Figure 4) in good agreement with single-crystal structure model.
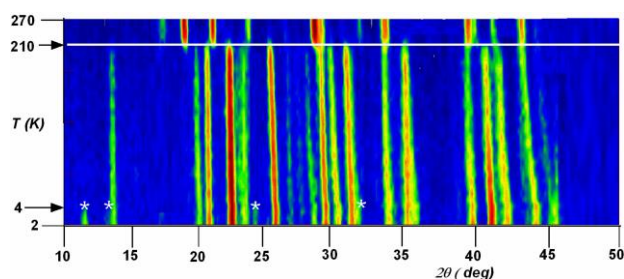
Figure 3. 2D contours of the temperature dependence of the D1B patterns between 270 and 2 K for [Emim][FeCl$_4$]. The (*) dots show the magnetic contributions. The line at 210 K shows the change of the crystalline structure.
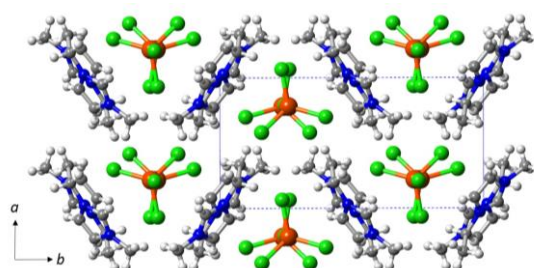

Figure 4. Crystal packing in the *a,b* plane of Emimim[FeCl$_4$] crystal structure at 270 K. Red (iron), green (chloride), black (carbon), blue (nitrogen) and white (hydrogen). The blue dashed square represent the unit cell.

A comparison of the D1B patterns for Emin[FeCl$_4$] (red) and its deuterated phase (blue) at 2 K is plotted in Figure 5. The data clearly show differences in the structural and magnetic peaks. Therefore, the intermolecular interactions between anions and cations (ionic, hydrogen bonding and van der Waals forces) are modified with the deuteration process. These forces affect the local- and long-range molecular ordering, which subsequently modify the magnetic couplings between an iron ion and its first shell of neighbouring iron ions changing the superexchange anion-anion interactions [14]. In order to try to resolve the low temperature crystal structure of both MILs, high-resolution neutron diffraction data at 10 K on D2B (λ = 1.594 Å) were collected (see Figure 6). A comparative view of

the patterns clearly shows a better signal/ratio in the deuterated phase and confirms the different low temperature crystal structures.

Only for the deuterated compound was found a satisfactory monoclinic crystal structure [M20 =16.8; F20 = 10.6] using the WINPLOTR programme [15], with unit cell parameters of a = 9.560 (1) Å, b =13.946 (1) Å, c = 14.460 (1) Å, β = 97.13(1). The analysis was consistent with the P2$_1$/m space group. The experimental, calculated and difference diffraction profiles are displayed in Figures 5 and 6 and the resolution of the crystal structure is now in progress. Focusing on the long-range magnetic ordering of the deuterated phase, below T$_N$, the additional magnetic peaks can be indexed with the propagation vector k = (0.5, 0, 0.5) (Figure 5), indicating that the magnetic unit cells is twice larger than the crystallographic one in a and c directions. This approach allows us to see some important differences when compared to Dimim[FeBr$_4$] analogous [6], in which the magnetic and nuclear unit cells are the same.
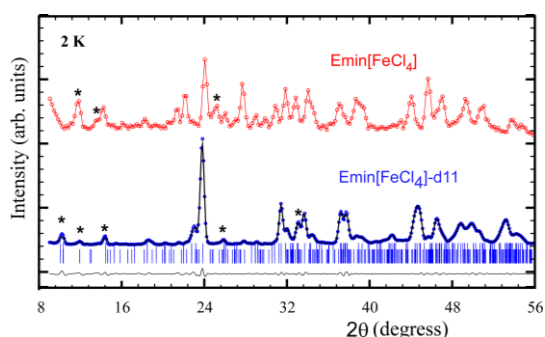
Figure 5. Neutron pattern for Emim[FeCl$_4$] and neutron diffraction profiles for the deuterated phase at 2 K obtained in D1B (λ = 2.52 Å). Positions of the magnetic (second row) profile are also presented. The (*) dots show the magnetic bragg peaks. The curves are shifted for clarity.
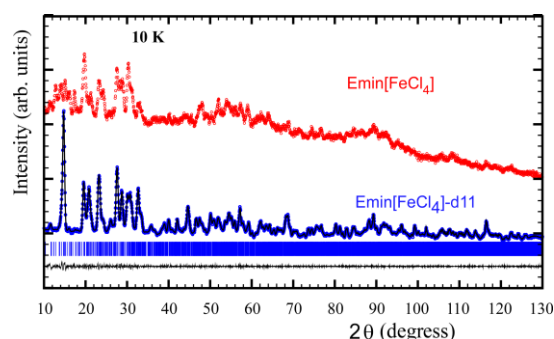
Figure 6. Neutron pattern for Emim[FeCl$_4$] and neutron diffraction profiles for the deuterated phase at 10 K obtained in D2B(λ = 1.594 Å). The curves are shifted for clarity.

3. Conclusions

Neutron data evidence a solid-solid transition in Emim[FeCl$_4$] near 210 K, this crystal structure being stable down to 2 K. The appearance of extra magnetic peaks below 4K in neutron diffraction data confirms the onset of a three-dimensional antiferromagnetic ordering. Finally, we have identified via magnetic and powder diffraction studies that these MILs change their magnetic behaviour with the deuteration process. The 3D antiferromagnetic ordering detected by magnetic measurements must take place via super-exchange coupling, the Fe−Cl···Cl−Fe interaction being the main exchange pathway. In addition, indirect exchange coupling of the type Fe-Cl···Im···Cl-Fe (Im = Imidazolium) could be present in both compounds. Taking in account that the strength of the magnetic exchange pathways via these super-exchange couplings depend on the following paramenters: (i) Cl ··· Cl distance, (ii) Fe− Cl ··· Cl −Fe angles and (iii) the Fe− Cl ··· Cl −Fe torsion angle (τ), these distances and angles should be quite similar, as inferred from the magnetic susceptibility measurements, being different their crystal structures. The present findings illustrates very well how small bonding-changes can have a profound effect on both crystal and magnetic structures of these materials whose framework is linked by non-covalent interactions.

4. Acknowledgements

5. References

[1] Okuhata M, Funasako Y, Takahashi K and Mochida T 2013 *Chem. Commun.* **49** 7662.

[2] Torimoto T, Tsuda T, Okazaki K and Kuwabata S 2010 *Adv. Mater.* **22** 1196.

[3] Santos J, Albo A and Irabien R 2014 *Soc. Chem. Adv.* **4** 40008.

[4] Steed, J W and Atwood J L *Supramolecular chemistry*. John Wiley & Sons: 2009.

[5] Dupont, J 2004 *J. Braz. Chem. Soc* **15** 341.

[6] García-Saiz A, de Pedro I, Migowski P, Vallcorba O, Junquera J, Blanco J A and Rodríguez Fernández, J 2014 *Inorg. Chem.* **53** 8384.

[7] Piecha-Bisiorek A, Jakubas R, Medycki W, Florek-Wojciechowska M, Wojciechowski M and Kruk D 2014. *J. Phys. Chem. A* **118** 3564.

[8] de Pedro I, Rojas D P, Albo J, Luis P, Irabien A, Blanco J A and Rodríguez Fernández, J 2010 *J. Phys.: Condens. Matter* **22(29)** 296006.

[9] de Pedro, I, Rojas D. P, Blanco J A and Rodríguez Fernández, J 2011 *J. Magn. Magn. Mater.* **323** 1254.

[10] Yoshida Y, Otsuka A, Saito G, Natsume S, Nishibori E, Takata M, Sakata M, Takahashi M and Yoko T 2005 *Bull. Chem. Soc. Jpn.* **78**, 1921.

[11] García-Saiz A, Migowski P, Vallcorba O, Junquera J, Blanco J. A, González J. A, Fernández-Díaz M. T, Rius J, Dupont J, Rodríguez Fernández J and de Pedro I 2014 *Chem. Eur. J.* **20** 72.

[12] García-Saiz A, de Pedro I, Blanco J A González J A and Rodríguez Fernández, J 2013 *J. Phys. Chem. B* **117** 3198.

[13] Bäcker T, Breunig O, Valldor M, Merz K, Vasylyeva V and Mudring A. V 2011 *Cryst. Growth & Design* **11(6)** 2564.

[14] García Saiz A, de Pedro I, Vallcorba O, Migowski P, Campo I, Barquin, L F, Abrahams I, Motevalli M, Dupont J, Gonzalez J A, Rodríguez Fernández, J 2015 *RSC Adv.* **5** 60835

[15] Roisnel T. and Rodriguez-Carvajal J 2000 WINPLOTR: A New Tool for Powder Difracction: Laboratoire Leon Brillouin (CEA-CNRS) Centre d'Etudes de Saclay, Gif sur Yvette Cedex, France.

[16] J. Rodríguez-Carvajal, J 1993 *Physica B* **192** 55 and later un-published versions; the programme is a strongly modified version of that described by Wiles D. B. and Young, R. A. 1981, *J. Appl. Crystallogr.* **14** 149.